Alqalam Journal of Medical and Applied Sciences. 2026;9(5):1268-1280
https://doi.org/10.54361/ajmas.269520

Original article

The Physicochemical and Antiplasmodial Properties of Microencapsulated Leaf Extract of *Carica Papaya* (Family: Caricaceae)

Yinka James Oyeniyi*, Irene Machi

Department of Pharmaceutics and Pharmaceutical Technology, Faculty of Pharmaceutical Sciences, Usmanu Danfodiyo University, Sokoto, Nigeria

Corresponding author: oyeniyi.yinka@udusok.edu.ng

Abstract

Malaria remains a major global health challenge, and there is growing interest in plant-derived antimalarial agents as alternative or adjunct therapies. Carica papaya has shown notable antiplasmodial activity; however, its therapeutic potential is limited by poor stability, variable bioavailability, and rapid release when used in crude form. Microencapsulation using biopolymer-based systems offers a promising strategy to improve the stability and controlled delivery of phytochemicals. This study aimed to develop and evaluate sodium alginate-based microencapsulated formulations of *Carica papaya* leaf extract to improve encapsulation efficiency, enable controlled release, and enhance in vivo antiplasmodial activity. Microcapsules were prepared via ionotropic gelation using different sodium alginate concentrations to create various formulations (IM_1, IM_2, and IM_3). The formulations were evaluated for encapsulation efficiency, morphology, swelling behavior, and in vitro drug release kinetics. The best-performing formulation (IM_3) was further tested for in vivo antiplasmodial activity using a Plasmodium berghei-infected Swiss albino mouse model. Parasitemia reduction was measured and compared with the crude extract, the negative control, and a standard antimalarial drug, and statistical analysis was conducted using appropriate significance tests ($p < 0.001$). The findings showed that polymer concentration significantly affected microcapsule properties, with IM_3 demonstrating the highest encapsulation efficiency, structural stability, and a sustained drug-release profile, while IM_2 exhibited a more balanced release pattern. In vivo studies indicated that the methanolic extract of Carica papaya significantly reduced parasitemia, with microencapsulated formulations showing markedly improved effectiveness. The IM_3 formulation produced the strongest antiplasmodial effect among the test groups and showed enhanced performance compared to the crude extract, with statistically significant differences ($p < 0.001$). Sodium alginate-based microencapsulation greatly improves the stability, controlled release, and antimalarial effectiveness of Carica papaya leaf extract. The IM_3 formulation demonstrates strong potential as a sustained-release phytopharmaceutical for malaria treatment, underscoring the importance of advanced formulation strategies in enhancing plant-derived therapeutic agents.

Keywords: *Carica papaya*, Microencapsulation, Sodium alginate, Anti-plasmodial activity.

Introduction

Malaria remains a major global health challenge, causing significant illness and death, especially in sub-Saharan Africa. The disease is caused by Plasmodium parasites transmitted by infected female Anopheles mosquitoes. The emergence of drug-resistant malaria strains has driven the search for alternative treatments [1-3]. Despite years of control efforts, malaria continues to be a serious public health issue due to socioeconomic factors, limited healthcare access, and climate conditions that promote mosquito breeding. Even more critically, the widespread appearance and increasing prevalence of Plasmodium strains resistant to common antimalarial drugs have greatly reduced the effectiveness of current treatments. This growing problem has heightened the urgency to develop new, safe, and effective therapies to supplement or replace existing antimalarial options.

Medicinal plants have long played a key role in treating malaria, especially in endemic areas where traditional medicine remains a vital part of primary healthcare. Carica papaya is a widely grown medicinal plant used for medicinal, cosmetic, and culinary purposes. The leaves are traditionally used as an antimalarial agent. Phytochemical screening has shown that the leaves contain various bioactive compounds, including alkaloids, flavonoids, phenolics, and terpenoids, which are believed to contribute to their antimalarial properties [4,5]. However, clinical use of C. papaya extract is limited by environmental degradation, rapid metabolism, and poor solubility. These issues reduce the effectiveness of the extract, calling for an advanced drug delivery system [6,7].

To overcome these limitations, advanced drug-delivery systems have gained increasing attention as promising strategies to improve the stability and effectiveness of plant-derived bioactive compounds. Among these methods, microencapsulation has become a successful technique for enhancing the delivery of phytochemicals. Microencapsulation involves trapping bioactive compounds within polymeric carriers, creating protective matrices that shield the encapsulated agents from environmental degradation and early metabolism. Furthermore, microencapsulation can enable controlled and sustained release of bioactive compounds, potentially increasing bioavailability, extending therapeutic effects, and reducing the frequency of dosing. As a result, microencapsulation technology offers a promising approach to enhance the antimalarial potential of Carica papaya extracts and support their development into effective

Received: *07-03-2026* - ***Accepted***: *06-05-2026* - ***Published***: *12-05-2026*

phytopharmaceutical formulations [8-11]. This study aimed to develop and evaluate the antiplasmodial activity of the microencapsulated *Carica. papaya* extract.

Materials and Methods

Materials

Leaves of Carica papaya were collected in Zuru town, within the Zuru Local Government Area of Kebbi State. The leaves were identified, assigned voucher number PCG/UDUS/Cari/0005, and then stored in the herbarium of the Department of Pharmacognosy and Ethnomedicine at Usmanu Danfodiyo University, Sokoto. All other reagents were of analytical grade

Extraction of Carica papaya leaf

The fresh leaves were air-dried, size-reduced, and sieved through a 600 µm mesh to obtain uniform particle sizes. Five hundred grams (500 g) of the powder was macerated with two liters (2 L) of 96% methanol for 5 days with constant agitation. The supernatant was decanted, filtered, concentrated using a rotary evaporator, and then dried to constant weight in a water bath maintained at 50°C [12]

Determination of absorption maxima and calibration equation for Carica papaya leaf extract

To determine the maximum absorption wavelength of the extract, a 1% W/V dispersion of the extract was prepared in 100 mL of phosphate buffer (pH 6.8). The dispersion was filtered through Whatman filter paper (0.5 µ), and the absorbance was measured using a UV-Visible spectrophotometer (Model Cintra 6, Type GBC UV–Visible, GBC, Scientific Equipment Ltd, Victoria, Australia) at different wavelengths. To obtain the calibration curve, the wavelength of maximum absorbance was used to scan five freshly prepared concentrations of the extract, and the resulting absorbance values were used to construct a Beer-Lambert plot [13]

Phytochemical screening of the Carica papaya leaf extract

Tests were conducted on the extract to detect alkaloids, flavonoids (alkaline test), saponins (foam test), tannins (ferric chloride test), cardiac glycosides (Keller-Killiani test), anthraquinones (Borntrager's test), carbohydrates (Molisch test and Fehling's test), and phenols (ferric chloride test) [14,15,16]

Fourier-transform infrared spectroscopy of Carica papaya leaf extract

The purpose of this investigation is to identify the functional groups present in the extract and to understand the possible secondary plant metabolites constituents of the plant extract [17.18]. In this study, a compressed disc of the extract was prepared with potassium bromide (KBr) and scanned using Fourier-transform infrared (FTIR) spectroscopy (spectrum BX 273, PerkinElmer, USA) in the range of 350 cm-1 to 4400 cm-1. The FTIR spectra were recorded, and the table-driven infrared application software (IRPal 2.0) was used to determine the class, structure, and functional group assignments based on the observed peak wavelengths. [19].

Microencapsulation of Carica papaya leaf Extract

Microcapsules were produced using the ionotropic gelation method. Ten grams (10 g) were uniformly dispersed in 5%, 7.5%, and 10% w/v sodium alginate solutions to create three formulations. Using a 10 mL syringe, the mixture was added dropwise to 500 mL of a 2% w/v calcium chloride solution while stirring continuously at 600 rpm. The gelled beads were cured for 30 minutes, then recovered by filtration, air-dried to a constant weight, and stored in a desiccator until needed [20,21,22,23]. The percentage yield was calculated using equation 1.

$$\%\text{Yield} = \frac{\text{Weight of microcapsules}}{\text{Weight of extract + calcium chloride + sodium alginate}} \times 100 \quad \ldots\ldots\ldots\ldots\ldots\ldots\ldots \quad .\text{EQ1}$$

Microcapsules Characterization

i. **Morphology**

Dried microcapsules were carefully mounted onto aluminum SEM stubs using double-sided conductive carbon tape to reduce aggregation and create a uniform monolayer. Loose particles were gently removed by taping. The mounted samples were sputter-coated with a thin layer of gold or a gold–palladium alloy in a vacuum to improve electrical conductivity and prevent charging. SEM imaging was carried out at 5–15 kV, with the working distance and magnification chosen to clearly visualize surface features. Micrographs were taken to evaluate particle shape, surface texture (smoothness, roughness, porosity), the presence of cracks or collapse, and the overall structural integrity of the microcapsules [24,25,26,27]

ii. **Mean particle size determination:**

The mean microcapsule size was determined from SEM micrographs using image analysis software (ImageJ). One hundred (100) randomly selected microcapsules were measured to ensure statistical reliability. For each particle, the diameter was measured (for non-spherical particles, the Feret diameter or the average of

Received*: 07-03-2026 -* ***Accepted****: 06-05-2026 -* ***Published****: 12-05-2026*

two perpendicular diameters was used), and the mean particle size ± standard deviation was calculated [28,29,30].

iii. **Swelling Index:**

The swelling index was determined as the weight gain after soaking 1 g in 100 mL of phosphate buffer (pH 6.8) for 12 hours [31,32]. The swelling index, expressed as a percentage, was calculated using equation 1:

$$\text{Swelling index (\%)} = \frac{FW - IW}{IW} \times 100 \quad \text{Eq 1}$$

where IW is the initial dry weight, and FW is the weight

iv. **Entrapment Efficiency**

One hundred milligrams (100 mg) of the microcapsules were precisely weighed and gently crushed to break the polymeric matrix. The crushed samples were transferred to a volumetric flask containing 200 mL of PBS (pH 6.8) and sonicated for 5 minutes to ensure complete extraction of the encapsulated herbal constituents. The resulting dispersion was centrifuged to remove insoluble polymeric material, and the clear supernatant was filtered. The concentration of the extracted herbal constituents was measured using spectrophotometry. Entrapment efficiency was determined by comparing the actual amount of extract recovered with the theoretical initial amount used in the formulation (equation 2) [33,34].

$$\text{Entrapment Efficiency (\%)} = \frac{\text{Actual Drug Content}}{\text{Theoretical Drug Content}} \times 100$$

v. **Drug release study:**

The dissolution profile of the microcapsules was investigated using the USP XXI Paddle apparatus operating at 100 rpm. The dissolution medium was phosphate buffer at pH 6.8, maintained at 37±0.5°C. Microcapsules equivalent to 250 mg of the extract were placed in the dissolution vessel. At regular intervals, 10 mL of the medium was withdrawn and replaced with an equal volume of fresh medium. The samples were filtered, diluted 1:9 with PBS at pH 6.8, and the amount of extract released was determined by UV spectroscopy at 220 nm [35,36].

vi. **Biological activity:**

Healthy Swiss albino mice *(Mus musculus)* were obtained from the Faculty of Veterinary Medicine, Usmanu Danfodiyo University, Sokoto, Nigeria. They were housed in standard mouse cages in the animal house of the Department of Pharmacology and Toxicology, Faculty of Pharmaceutical Sciences, Usmanu Danfodiyo University, Sokoto, and were allowed two weeks to acclimatize before the start of the experiments. All animals were handled according to the international guiding principles for Biomedical Research involving Animals [14], as permitted by the Usmanu Danfodiyo University, Sokoto, ethical committee concerning the use of laboratory animals.

The in vivo anti-parasitemia activity of IM_3 (the optimized microencapsulated formulation) was evaluated using a murine malaria model. Healthy Swiss albino mice (18–25 g) were intraperitoneally infected with about 1×10^7 Plasmodium berghei-infected erythrocytes obtained from a donor mouse at the Center for Advanced Medical Research and Training, Usmanu Danfodiyo University, Sokoto. Following infection, animals were randomly divided into experimental groups receiving: vehicle (negative control), standard antimalarial therapy (artesunate, 5 mg/kg/day), crude methanolic extract of Carica papaya (CRD), or graded doses of the microencapsulated formulation (IM_3: 100, 200, and 400 mg/kg). Treatments were given orally once daily for three consecutive days (Day 0–Day 3), following standard 4-day suppressive test protocols.

Parasitemia levels were assessed by microscopic examination of Giemsa-stained thin blood smears prepared from tail-vein samples. The percentage parasitemia was determined by counting infected erythrocytes relative to the total erythrocyte count, while the percentage chemosuppression was calculated relative to the negative control.

All data were expressed as mean ± standard error of the mean (SEM). Statistical analysis was conducted using one-way analysis of variance (ANOVA), followed by Tukey's post hoc multiple comparison test. Statistical significance was set at $p < 0.05$. [37,38].

Results and discussion

The Yield

The percentage yield of an extract is a fundamental quantitative parameter in phytochemical and pharmaceutical research because it reflects the efficiency of the extraction process and the potential availability of bioactive constituents for further analysis or formulation [39]. In this study, 49.09 g of extract was obtained from 500 g of the crude drug, corresponding to a percentage yield of 9.82%. Compared with similar studies, this yield falls within the typical range for aqueous or hydroalcoholic extractions of plant materials, which often produce yields between 5% and 15%, depending on the plant species and solvent system [40].

Received*: 07-03-2026 -* ***Accepted****: 06-05-2026 -* ***Published****: 12-05-2026*

The Absorption Maxima of Carica papaya Leaf Extract

The spectrophotometric analysis revealed that Carica papaya leaf extract exhibits a main absorption maximum at 280 nm, with an absorbance of 0.68, as shown in Figure 1. A clear absorption maximum is important for studying the entrapment efficiency and dissolution profile of Carica papaya microcapsules.

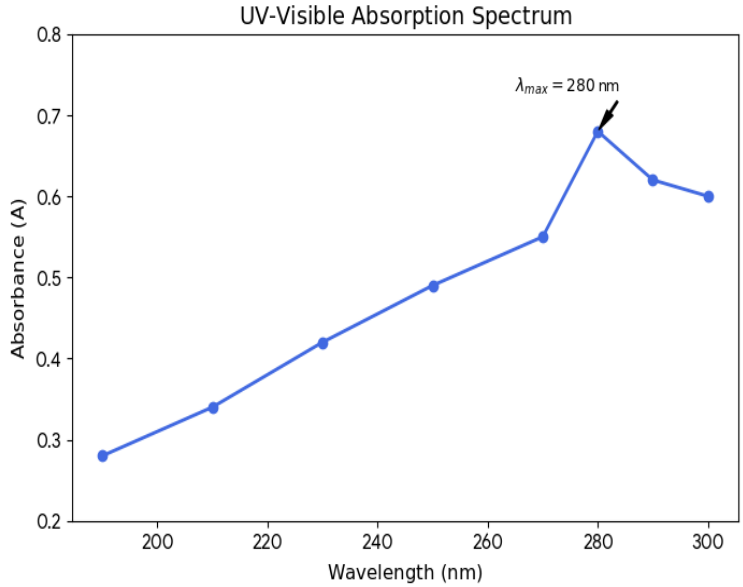

Figure 1: UV-Visible absorption spectrum of Carica papaya extract

Phytochemical Screening

The results of phytochemical screening indicate that the Carica papaya methanolic extract is rich in secondary metabolites, including tannins, alkaloids, saponins, carbohydrates, cardiac glycosides, triterpenoids (steroids), phenols, and flavonoids. These were further confirmed by the FTIR spectroscopy results, as shown in Figure 2 and Table 1.

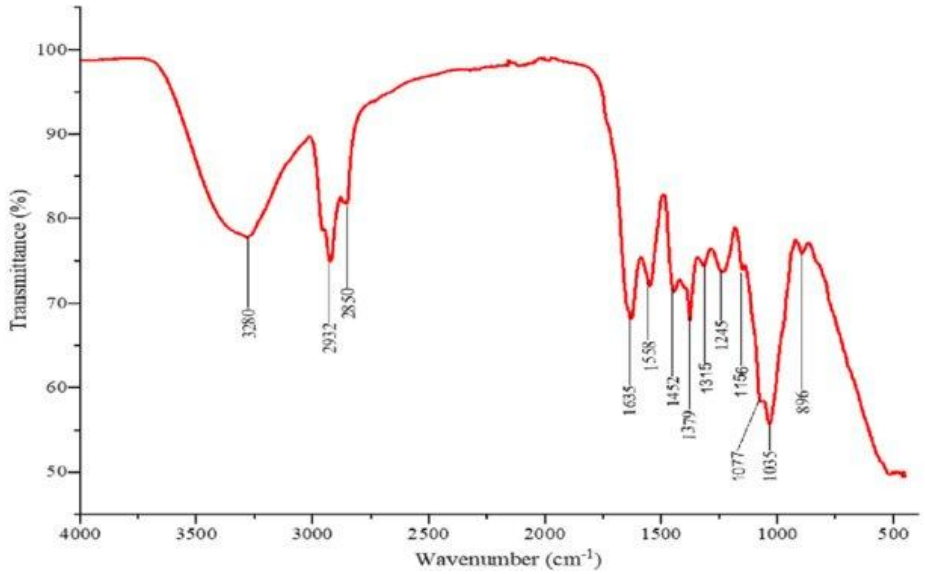

Figure 2: FT-IR of Carica papaya Leaves Extract

Table 1. Identify peaks and Corresponding Functional Group

FTIR Peak (cm^{-1})	Functional Group	Possible Phytochemical Source	Interpretation
3280–3400	O–H stretching	Phenols, alcohols, flavonoids	Indicates hydrogen-bonded hydroxyl groups present in polyphenolic compounds
2932, 2850	C–H stretching	Alkanes, lipids, terpenoids	Suggests the presence of long hydrocarbon chains
1630–1650	C=C or C=O stretching	Amides, flavonoids, proteins	Associated with conjugated double bonds or amide groups

Received*: 07-03-2026 -* ***Accepted****: 06-05-2026 -* ***Published****: 12-05-2026*

1550–1560	N–H bending	Alkaloids or amide II band	Indicates nitrogen-containing compounds
1450–1380	CH_2/CH_3 bending	Phenolic compounds, lignin	Suggests aromatic ring vibrations
1240–1260	C–O stretching	Phenols, esters	Indicates phenolic esters or ether groups
1030–1150	C–O–C stretching	Glycosides, carbohydrates	Suggests the presence of sugar moieties

Microcapsule Yield

Three Carica papaya microcapsule formulations were prepared with sodium alginate concentrations of 5% (IM_1), 7.5% (IM_2), and 10% (IM_3). The yield percentages of these formulations, ranging from 42.88% to 68.88%, were measured to assess microcapsule formation efficiency. The microcapsule yield ranking is $IM_3 \geq IM_2 \geq IM_1$. These results indicate that higher concentrations of the wall-forming polymer enhance the structural strength of the microcapsules, likely due to a stronger gel network formed during cross-linking [41,42].

Table 2: Percentage Yield of Carica papaya Microcapsule Formulations Prepared by Ion Gelation Technique

Formulation	Sodium alginate (% w/v)	Yield (%)
IM_1	5.0	42.88
IM_2	7.5	52.87
IM_3	10.0	68.88

These findings suggest that optimizing the wall material concentration is critical to improving microcapsule production efficiency. Increasing sodium alginate concentration increases the polymer solution's viscosity, promoting the formation of a stable gel matrix during ionotropic gelation with calcium chloride, thereby improving encapsulation efficiency and overall yield [43,44].

Microcapsule Morphology

The microcapsule formulations (IM_1, IM_2, and IM_3) exhibited predominantly spherical morphology, as shown in Figure 3, which is a critical quality attribute in microencapsulation systems due to its influence on flowability, packing efficiency, and drug release kinetics. Spherical particles are generally associated with improved uniformity and predictable performance in drug delivery systems [45].

Figure 3: Macroscopic Appearance of Microcapsule Formulations

The morphology of microcapsules was significantly influenced by sodium alginate concentration, with higher concentration leading to improved structural properties. At the lowest concentration, IM_1 formulations were relatively small and exhibited lower rigidity, with occasional surface irregularities, likely due to an insufficient polymer network that failed to maintain structural integrity. However, in formulation IM_2, the particles showed enhanced sphericity and smoother surfaces, indicating more efficient polymer entanglement and cross-linking. The most optimal morphology was observed in IM_3, where the microcapsules exhibited a uniform spherical shape with compact, smooth surfaces; this is attributed to the increased solution viscosity, which facilitates better droplet formation and creates a robust, low-porosity gel

Received: *07-03-2026* - ***Accepted***: *06-05-2026* - ***Published***: *12-05-2026*

matrix. These findings are consistent with established research, which notes that higher alginate concentrations enhance the mechanical strength and stability of encapsulation systems [46,47].

Particle Size, Swelling Index, and Entrapment Efficiency

The values for the particle size, swelling index after 24 hours, and the entrapment efficiency of microcapsules are shown in Table 3. PS and EE values show a direct proportionality with sodium alginate concentration, whereas SI shows an inverse relationship. This can be attributed to the increase in solution viscosity at higher alginate concentrations, which leads to the formation of larger droplets during ionotropic gelation. Increased viscosity limits droplet breakup and promotes the formation of larger, more spherical microcapsules. Similar observations have been reported in alginate-based encapsulation systems, where polymer concentration significantly influences microcapsule size and structural properties [48,49]

Table 3: The particle size (PS), Swelling Index (SI), and Entrapment Efficiency (EE) of C. Papaya Microcapsules

Parameters	IM_1	IM_2	IM_3
PS (mm) ±SD	1.33	1.48	1.62
SI (%)	89.49	74.89	68.79
EE (%)	65.09	72.68	74.88

In contrast, the swelling index decreased from 89.49% (IM_1) to 68.79% (IM_3), indicating that higher sodium alginate concentrations reduce water uptake. This behavior is likely due to the formation of a denser, more highly crosslinked polymer network, which restricts water diffusion into the microcapsules. The reduced swelling at higher concentrations suggests enhanced structural integrity and lower porosity of the gel matrix. Conversely, entrapment efficiency increased significantly from 65.09% (IM_1) to 74.88% (IM_3), indicating that higher polymer concentrations enhance the system's encapsulation capacity. The increased viscosity and matrix density reduce the diffusion of the extract into the external phase during gelation, thereby minimizing loss and enhancing retention within the microcapsules. These findings are consistent with previous studies, which report a direct relationship between polymer concentration and encapsulation efficiency due to improved matrix formation and reduced drug leakage [50,51].

Dissolution and Release Kinetics of Carica papaya Microcapsules

The dissolution profiles for the three formulations are presented in Figure 4. It was observed that there is a clear concentration-dependent drug release behavior typical of polymeric microcapsule systems, particularly those formulated with sodium alginate [52,53]. IM_1 exhibited the fastest release, reaching approximately 99.6% of the drug release within 120 min, indicating a relatively weak polymeric matrix that allows rapid penetration of the dissolution medium and faster diffusion of the encapsulated drug. In contrast, IM_2 exhibited a more gradual, sustained release pattern, achieving complete release at 300 min, suggesting an optimal polymer concentration that balances structural integrity with controlled diffusion. IM_3 exhibited the prolonged release profile, reaching 89.8% at 300 min, which can be attributed to a denser, more cross-linked polymer network that restricts solvent ingress and drug diffusion. This trend is consistent with the known behavior of alginate-based systems, where increasing polymer concentration enhances gel strength and reduces drug mobility within the matrix [54,55]. IM_2 and IM_3 will be useful in formulating a prolonged and sustained release oral formulation, solving the problem of adherence to medication, a key factor in drug therapy failure (DTF), while IM_1 will be more clinically relevant in cases where a faster onset of drug therapy is desired [56]

Received*: 07-03-2026 -* ***Accepted****: 06-05-2026 -* ***Published****: 12-05-2026*

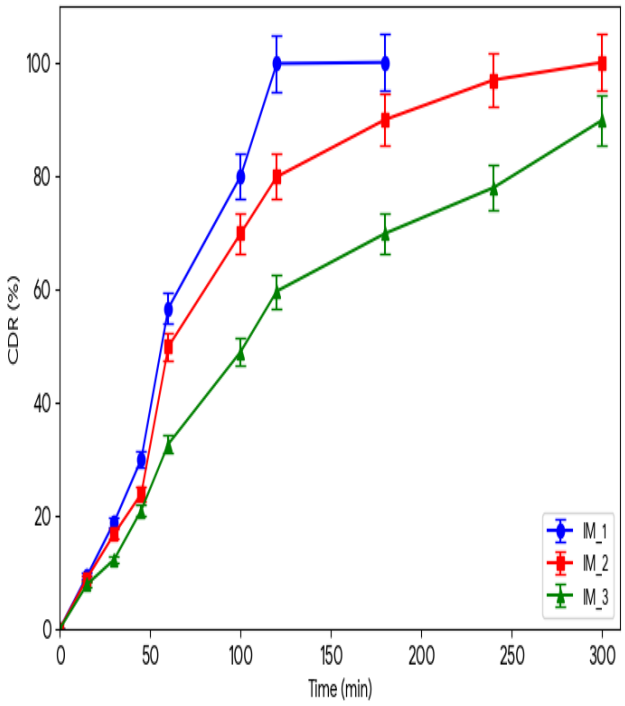

Figure 4: Percentage Cumulative Drug Released

The release curves further indicate a biphasic release mechanism: an initial moderate release phase (0–60 min), followed by a sustained diffusion-controlled phase. The absence of a pronounced burst effect suggests efficient encapsulation and uniform drug distribution within the microcapsules. The sustained release observed, especially in IM_2 and IM_3, is characteristic of diffusion-controlled systems described by the Higuchi and Korsmeyer–Peppas models (Table 4), in which drug release is governed primarily by matrix swelling and diffusion through the hydrated polymer network. IM_3 exhibited a prolonged-release profile, reaching 89.8% cumulative drug release at 300 min, indicating sustained liberation of the drug over time. Meanwhile, the high Korsmeyer–Peppas correlation coefficient (R^2 = 0.998) suggests that the release kinetics closely fit the Korsmeyer–Peppas model, implying that diffusion was the dominant mechanism controlling drug release. Therefore, the prolonged release observed for IM_3 is not contradictory to the kinetic modeling results; rather, it indicates that the sustained-release behavior was primarily governed by diffusion through the polymer matrix. This behavior aligns with reports that alginate microcapsules exhibit delayed and controlled release due to swelling-induced diffusion mechanisms, with release rates decreasing as polymer density increases. [57, 58].

Table 4. Release kinetics of Carica papaya Microcapsules

Formulations	Zero Order R^2	First Order R^2	Higuchi R^2	Korsmeyer-Peppas R^2
IM_1	0.835	0.901	0.919	0.9346
IM_2	0.811	0.882	0.948	0.995
IM_3	0.789	0.899	0.979	0.998

Biological Activity

The anti-plasmodial activity of the methanolic extract of Carica papaya was evaluated in Plasmodium berghei-infected mice and expressed as the percentage of parasite suppression relative to the untreated infected control group. The results demonstrated a clear time and dose-dependent antimalarial effect across all treated groups [61,62].

Received*: 07-03-2026 -* ***Accepted****: 06-05-2026 -* ***Published****: 12-05-2026*

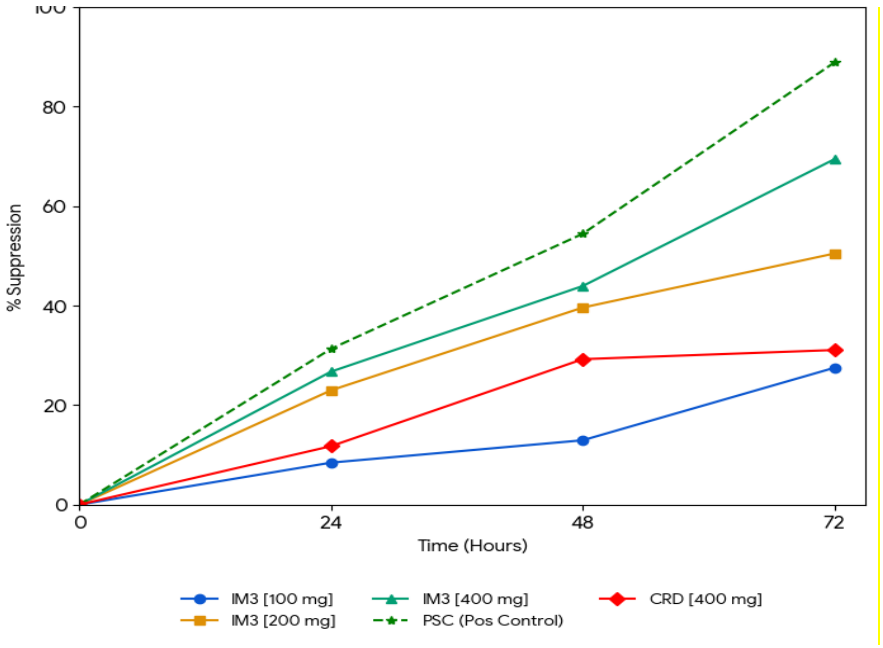

Figure 5: Percentage Suppression of Parasitaemia

As shown in Table 5, all treatment groups exhibited progressive suppression of parasites over the 72-hour observation period. The IM_3 formulations showed a clear dose-dependent response, with suppression increasing as the dose rose from 100 mg/kg to 400 mg/kg. At 72 hours, IM_3 [400 mg/kg] achieved 69.37 ± 2.28% parasite suppression, compared with 50.43 ± 3.22% for IM_3 [200 mg/kg] and 27.48 ± 2.32% for IM_3 [100 mg/kg]. This represents a strong dose–response relationship (R^2 = 0.941), indicating high predictive consistency of the formulation's pharmacological effect [63]. The antiplasmodial activity is linked to bioactive secondary metabolites such as flavonoids and alkaloids (notably carpaine), which disrupt hemoglobin digestion and parasite fatty acid biosynthesis pathways [64,61].

TABLE 5: Percent Parasite Suppression of C. papaya Extract Against P. berghei

Time (Hrs)	IM_3 [100 mg]	IM_3 [200 mg]	IM_3 [400 mg]	PSC	CRD [400 mg]	NGC
0	0	0	0	0	0	0
24	8.43 ± 2.21	22.96 ± 3.28	26.71 ± 2.42	31.30 ± 2.18	11.74 ± 2.38	0
48	12.92 ± 2.28	39.58 ± 2.44	43.90 ± 1.23	54.40 ± 2.58	29.21 ± 2.42	0
72	27.48 ± 2.32	50.43 ± 3.22	69.37 ± 2.28	88.80 ± 2.22	31.05 ± 2.48	0

Key: CRD = Crude extract, NGC = Negative control, PSC = Positive Control

A notable finding from this study is the marked superiority of the microencapsulated IM_3 formulation over the crude extract at equivalent doses. At 400 mg/kg, IM_3 achieved 69.37% parasite suppression, whereas the crude extract (CRD) produced only 31.05% suppression. This represents more than a two-fold increase in efficacy and was statistically significant ($p < 0.001$), indicating enhanced pharmacological performance of the formulated product. The improved activity of IM_3 may be attributed to enhanced bioavailability, protection of phytoconstituents from degradation, and improved release characteristics enabled by microencapsulation. These factors likely increase systemic exposure to active metabolites, thereby enhancing antiplasmodial efficacy. [63,65].

Received*: 07-03-2026 -* ***Accepted****: 06-05-2026 -* ***Published****: 12-05-2026*

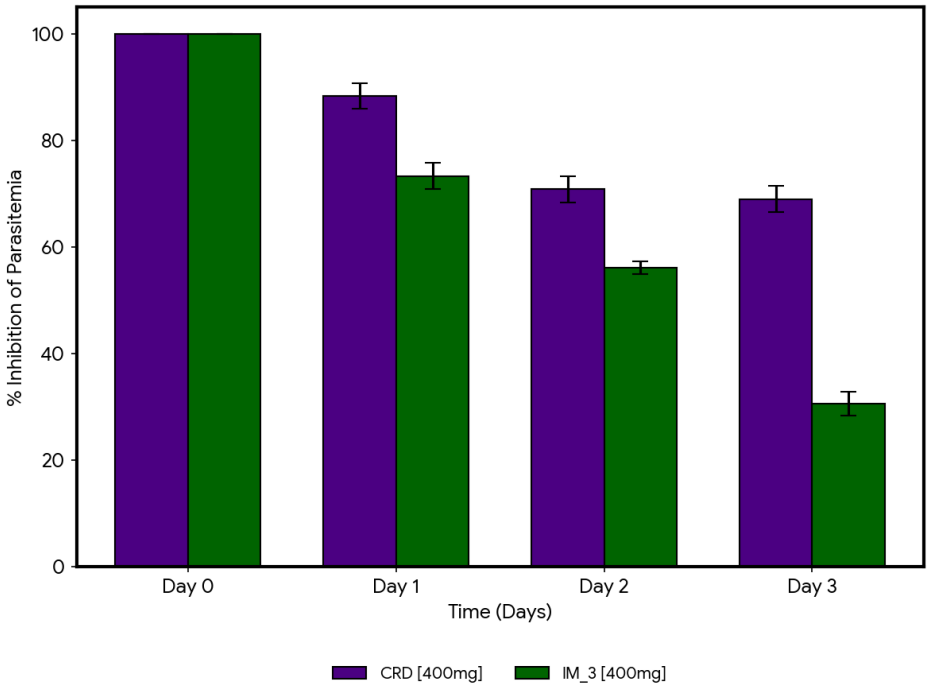

Figure 5: Comparative Anti-plasmodial activity of crude extract and IM_3 (encapsulated) at the same dose

The increased effectiveness of IM_3 is closely linked to the dual roles of microencapsulation: protecting phytochemicals and enabling controlled-release delivery. Encapsulation likely shields sensitive compounds from acidic breakdown and enzymatic processes, thereby enhancing systemic bioavailability [65]. This process is especially important for Carica papaya phytoconstituents, which are vulnerable to rapid first-pass metabolism [62]. Additionally, encapsulation promotes sustained drug release, providing extended therapeutic exposure that is crucial for disrupting the 24-hour erythrocytic cycle of Plasmodium berghei. As shown in Figure 6, formulation IM_3 maintained a stable inhibitory effect over the 72-hour period, while the crude extract experienced a quick decline in activity. This persistent pharmacodynamic response supports previous findings that encapsulated plant-based formulations improve therapeutic consistency and effectiveness [65]. Furthermore, enhanced lipophilicity and cellular permeability may help bioactive compounds enter infected erythrocytes more easily, allowing for better interaction with intracellular parasite targets.

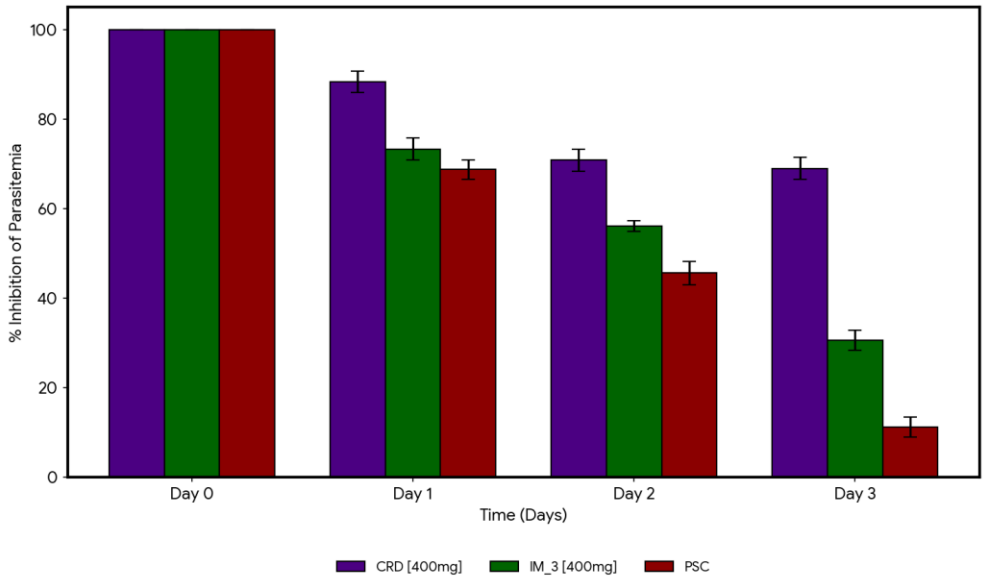

Figure 6: Comparative Anti-plasmodial activity of crude extract, IM_3 (encapsulated), artesunate (PSC)

Received*: 07-03-2026 -* ***Accepted****: 06-05-2026 -* ***Published****: 12-05-2026*

Table 6: Percentage of Total Reduction of Parasitaemia

Treatment Group	Dose (mg/kg)	% Parasite Suppression at 72 h	Total Reduction of Parasitaemia (%)
IM_3	100	27.48 ± 2.32	27.48 ± 2.32
IM_3	200	50.43 ± 3.22	50.43 ± 3.22
IM_3	400	69.37 ± 2.28	69.37 ± 2.28
PSC	5mg/kg	88.80 ± 2.22	88.80 ± 2.22
CRD	400	31.05 ± 2.48	31.05 ± 2.48
NGC	—	0	0

Values represent percentage parasite suppression at 72 hours relative to the untreated infected control group (NGC). Total reduction of parasitaemia was calculated using the standard in vivo antimalarial endpoint method, where higher values indicate greater chemotherapeutic efficacy. Although artesunate (PSC) remained the most potent treatment, achieving 88.80% parasitemia clearance, the IM_3 fraction showed a similar inhibitory trend, indicating partial convergence toward standard antimalarial pharmacodynamics. This aligns with evidence that combination or improved delivery systems involving Carica papaya may enhance therapeutic outcomes and potentially act synergistically with conventional drugs [66]. However, artesunate consistently outperformed all plant-derived treatments, confirming its superior pharmacological potency. In contrast, the negative control group showed a steady increase in parasitemia, reaching approximately 140% of baseline by Day 3 ($p < 0.001$ vs treated groups), confirming active infection progression and supporting the pharmacological effects seen in the treatment groups [62,65,68].

Conclusion

This study established sodium alginate-based microencapsulation as an effective and tunable delivery system for *Carica papaya* leaf extract, with polymer concentration playing a critical role in determining encapsulation efficiency, particle morphology, swelling behavior, and drug release kinetics. Among the formulations developed, IM_3 demonstrated the highest encapsulation efficiency, superior structural integrity, and sustained-release characteristics, making it particularly suitable for extended-release applications, while IM_2 exhibited a more balanced release profile, appropriate for controlled therapeutic delivery with a moderate onset and prolonged action. In vivo evaluation confirmed that the methanolic extract of *Carica papaya* possesses significant antiplasmodial activity, which is markedly enhanced by microencapsulation, particularly in the IM_3 formulation. The results showed strong dose-dependent efficacy with highly significant differences between treatment groups ($p < 0.001$), and the encapsulated formulations consistently outperformed the crude extract, with IM_3 approaching the inhibitory profile of artesunate. Overall, the findings demonstrate that ionotropic gelation using sodium alginate is a robust pharmaceutical strategy for improving the stability, bioavailability, and therapeutic performance of plant-derived bioactives. Microencapsulation not only optimized drug release behavior but also significantly enhanced antimalarial efficacy, underscoring the importance of formulation engineering in phytomedicine development. These results position the IM_3 formulation as a promising extended-release antimalarial candidate, while also highlighting the broader potential of encapsulated *Carica papaya* extracts as supportive or adjunct therapies in malaria management.

Conflict of interest. Nil

References

1. World Health Organization. Malaria fact sheet [Internet]. Geneva: World Health Organization; 2025 [cited 2026 Apr 27]. Available from: https://www.who.int/news-room/fact-sheets/detail/malaria
2. United Nations Office at Geneva. Malaria: Drug resistance and underfunding threaten progress towards eliminating the killer disease [Internet]. Geneva: United Nations; 2025 Dec 4 [cited 2026 Apr 27]. Available from: https://www.ungeneva.org/en/news-media/news/2025/12/113596/malaria-drug-resistance-and-underfunding-threaten-progress-towards
3. Theodoridis L, Carvalho TG. Antimalarial drug resistance and drug discovery: Learning from the past to innovate the future. Int J Parasitol Drugs Drug Resist. 2025. https://doi.org/10.1016/j.ijpddr.2025.100602.
4. Hlatshwayo S, Thembane N, Krishna SBN, Gqaleni N, Ngcobo M. Extraction and Processing of Bioactive Phytoconstituents from Widely Used South African Medicinal Plants for the Preparation of Effective Traditional Herbal Medicine Products: A Narrative Review. Plants. 2025;14(2):206.**https://doi.org/10.3390/plants14020206**
5. Sanjai C, Gaonkar SL, Hakkimane SS. Harnessing Nature's Toolbox: Naturally Derived Bioactive Compounds in Nanotechnology-Enhanced Formulations. ACS Omega. 2024 Oct 18;9(43):43302-43318. https://doi.org/10.1021/acsomega.4c07756.
6. Singh SP, Kumar S, Mathan SV, Tomar MS, Singh RK, Verma PK, et al. Therapeutic application of Carica papaya leaf extract in the management of human diseases. Daru. 2020 Dec;28(2):735-744. https://doi.org/10.1007/s40199-020-00348-7.

Received: *07-03-2026* - ***Accepted***: *06-05-2026* - ***Published***: *12-05-2026*

7. Evbuomwan IO, Stephen Adeyemi O, Oluba OM. Indigenous medicinal plants used in folk medicine for malaria treatment in Kwara State, Nigeria: an ethnobotanical study. BMC Complement Med Ther. 2023 Oct 19;23(1): 324. https://doi.org/10.1186/s12906-023-04131-4.
8. Valenzuela Villela KS, Alvarado Araujo KV, Garcia Casillas PE, Chapa González C. Protective encapsulation of a bioactive compound in starch–polyethylene glycol-modified microparticles: Degradation analysis with enzymes. Polymers (Basel). 2024 Jul 12;16(14): 2075. https://doi.org/10.3390/polym16142075.
9. Hamid S, Moussa H, Mahdjoub MM, Berrabah I, Djihad N, Attia A, et al. Biopolymer-Based Microencapsulation of Bioactive Compounds: Evaluation of the Impact of Encapsulated Compound Characteristics on Process Efficiency. Surfaces. 2025;8(1):15. https://doi.org/10.3390/surfaces8010015.
10. Laureanti EJG, Paiva TS, de Matos Jorge LM, Jorge RMM. Microencapsulation of bioactive compound extracts using maltodextrin and gum arabic by spray and freeze-drying techniques. Int J Biol Macromol. 2023 Dec 1;253(Pt 4):126969. https://doi.org/10.1016/j.ijbiomac.2023.126969
11. Szpicer A, Bińkowska W, Stelmasiak A, Wojtasik-Kalinowska I, Czajkowska A, Mierzejewska S, et al. Innovative Microencapsulation Techniques of Bioactive Compounds: Impact on Physicochemical and Sensory Properties of Food Products and Industrial Applications. Appl Sci. 2025;15(22):11908. https://doi.org/10.3390/app152211908.
12. Myo H, Khat-Udomkiri N. Optimization of ultrasound-assisted extraction of bioactive compounds from coffee pulp using propylene glycol as a solvent and their antioxidant activities. Ultrason Sonochem. 2022 Sep;89:106127. https://doi.org/10.1016/j.ultsonch.2022.106127.
13. Wathudura P, Pham H, Siriwardana K, Athukorale S, Jayasundara U, Gunatilake SR, et al. Expanding the horizons of UV–vis spectroscopy education: Beyond the Beer–Lambert law. J Chem Educ. 2025;102(6):2389-2397. https://doi.org/10.1021/acs.jchemed.5c00255.
14. Phuyal A, Ojha PK, Guragain B, et al. Phytochemical screening, metal concentration determination, antioxidant activity, and antibacterial evaluation of Drymaria diandra plant. Beni-Suef Univ J Basic Appl Sci. 2019;8(1):16. https://doi.org/10.1186/s43088-019-0020-1.
15. Ahmed Z, Aziz S, Hanif M, et al. Phytochemical screening and enzymatic and antioxidant activities of Erythrina suberosa (Roxb) bark. J Pharm Bioallied Sci. 2020 Apr-Jun;12(2):192-200. https://doi.org: 10.4103/jpbs.JPBS_222_19.
16. Andrich B, Pollo L, Bueno PR, Yu GFB. Phytochemical Screening. protocols.io. 2025. https://doi.org/10.17504/protocols.io.bp2l6zb85gqe/v1.
17. Pasieczna-Patkowska S, Cichy M, Flieger J. Application of Fourier Transform Infrared (FTIR) Spectroscopy in Characterization of Green Synthesized Nanoparticles. Molecules. 2025;30(3):684. https://doi.org/10.3390/molecules30030684.
18. Al-Amin K, Kawsar M, Mamun MTRB, Sahadat Hossain M. Fourier transform infrared spectroscopic technique for analysis of inorganic materials: a review. Nanoscale Adv. 2025;7(21):6677-6702. https://doi.org/10.1039/d5na00522a.
19. Liu Z, Ding H, Zhao S, Wang H, Xu Y. Exploring the Hyperspectral Response of Quercetin in Anoectochilus roxburghii (Wall.) Lindl. Using Standard Fingerprints and Band-Specific Feature Analysis. Plants (Basel). 2025;14(20):3141. https://doi.org/10.3390/plants14203141.
20. Abdulkadhim SL, Mohamed MBM, Salman AMH. Effect Of Different Variables on the Formulation Of Sodium Alginate Beads. AJPS. 2024;24(2):117-126. https://doi.org/10.32947/ajps.v24i2.1007
21. Naranjo-Durán AM, Quintero-Quiroz J, Rojas-Camargo J, et al. Modified-release of encapsulated bioactive compounds from annatto seeds produced by optimized ionic gelation techniques. Sci Rep. 2021 Jan 12;11(1):1317. https://doi.org/10.1038/s41598-020-80119-1.
22. Toprakçı İ, Torun M, Şahin S. Development of an Encapsulation Method for Trapping the Active Materials from Sour cherry Biowaste in Alginate Microcapsules. Foods. 2023 Jan;12(1):130. https://doi.org/10.3390/foods12010130.
23. Cui P, Zhou J, Xiao X, et al. Preparation and properties of walnut oil microcapsules. LWT. 2025; 225:117853. https://doi.org/10.1016/j.lwt.2025.117853.
24. Fallahasghari EZ, Højgaard Lynge M, Espholin Gudnason E, Munkerup K, Mendes AC, Chronakis IS. Carbohydrate Core–Shell Electrosprayed Microcapsules for Enhanced Oxidative Stability of Vitamin A Palmitate. Pharmaceutics. 2023 Oct 30;15(11):2633. https://doi.org/10.3390/pharmaceutics15112633.
25. Shah S, Zhang FR, Ge YW, et al. Microcapsules of mesoporous silica and cyclodextrin modified loaded with nonanal and decanal for effective control of Sitotroga cerealella in grain storage environments. Pest Manag Sci. 2024 Jun;80(6):2668-2678. https://doi.org/10.1002/ps.7973
26. Lai H, Liu Y, Huang G, et al. Fabrication and antibacterial evaluation of peppermint oil-loaded composite microcapsules by chitosan-decorated silica nanoparticles stabilized Pickering emulsion templating. Int J Biol Macromol. 2021 Aug 1;183:2314-2325. https://doi.org/10.1016/j.ijbiomac.2021.05.198.
27. Seyrekoğlu F, Temiz H, Eser F, et al. Optimization of Hypericum Perforatum Microencapsulation Process by Spray Drying Method. AAPS PharmSciTech. 2024 Apr 11;25(4):99. https://doi.org/10.1208/s12249-024-02820-y.
28. Menuel S, Saitzek S, Monflier E, Hapiot F. Particle size effect in the mechanically assisted synthesis of β-cyclodextrin mesitylene sulfonate. Beilstein J Org Chem. 2020 Oct 22;16:2598-2606. https://doi.org/10.3762/bxiv.2020.72.v1
29. Debut A, Vizuete K, Pazmiño K. Effect of Visual Cognition on the Measurement of Particle Size Using ImageJ Software. Curr Mater Sci. 2021;14(2):142-148. https://doi.org/10.2174/2666145414666210421080113
30. Díaz-García V, Haensgen A, Inostroza L, Contreras-Trigo B, Oyarzun P. Novel Microsynthesis of High-Yield Gold Nanoparticles to Accelerate Research in Biosensing and Other Bioapplications. Biosensors (Basel). 2023 Nov 21;13(12):992. **https://doi.org/10.3390/bios13120992**

Received: *07-03-2026* - ***Accepted***: *06-05-2026* - ***Published***: *12-05-2026*

31. De Piano R, Caccavo D, Barba AA, Lamberti G. Swelling Behavior of Anionic Hydrogels: Experiments and Modeling. Gels. 2024 Dec 11;10(12):813. https://doi.org/10.3390/gels10120813.
32. Irfan J, Ajaz Hussain M, Muhammad TH, et al. A pH-sensitive, stimuli-responsive, superabsorbent, smart hydrogel from psyllium (Plantago ovata) for intelligent drug delivery. RSC Adv. 2021 Jun 4;11(32):19755-19767. https://doi.org/10.1039/D1RA02219A.
33. Khatoon M, Ali A, Hussain MA, Haseeb MT, Sher M, Alsaidan OA, et al. A superporous and pH-sensitive hydrogel from Salvia hispanica (chia) seeds: stimuli responsiveness, on-off switching, and pharmaceutical applications. RSC Adv. 2024;14(38):27764-27776. https://doi.org/10.1039/d4ra04770b.
34. Zhao J, Qin X, Liu Y, He Q, Qin J, Shen F, et al. Comparative Evaluation of Spray-Drying Versus Freeze-Drying Techniques on the Encapsulation Efficiency and Biofunctional Performance of Chenpi Extract Microcapsules. Foods. 2025 May 15;14(10):1825. https://doi.org/10.3390/foods14101825.
35. Adeyemi JJ, Ajayi AM, Ajala KA,.Alginate-based microencapsulation enhances antinociceptive and anti-inflammatory activities of Phyllanthus amarus and Phyllanthus muellerianus. Food Hydrocoll Health. 2024;6:100190. https://doi.org/10.1016/j.fhfh.2024.100190.
36. Singh M, Ullapu PR, Mariadoss AVA, Kumar S, Kang SG. Development of pH-Sensitive Multiparticulates for Orally Disintegrating Tablets of Proton Pump Inhibitors: Physicochemical Characterization and Drug Release Studies. Pharmaceutics. 2025 Sep 1;17(9):1187. **https://doi.org/10.3390/pharmaceutics17091187**
37. Fouad SA, Abdelaziz N, Teaima MH, et al. Engineering orally disintegrating tablets for buccal delivery of cilostazol with enhanced dissolution and bioavailability: a novel dual porogenic approach, in vitro characterization, and in vivo evaluation in rats. Pharm Dev Technol. 2025;30(3):280-294. https://doi.org/10.1080/10837450.2025.2472887
38. Melariri P, Campbell W, Etusim P, Smith P. Antiplasmodial Properties and Bioassay-Guided Fractionation of Ethyl Acetate Extracts from Carica papaya Leaves. J Parasitol Res. 2011;2011:104954. https://doi.org/10.1155/2011/104954.
39. Hawadak J, Chaudhry S, Pande V, Singh V. Comparison of SYBR green I and lactate dehydrogenase antimalarial in vitro assay in Plasmodium falciparum field isolates. J Pharmacol Toxicol Methods. 2023;124:107472. https://doi.org/10.1016/j.vascn.2023.107472.
40. Nortjie E, Basitere M, Moyo D, Nyamukamba P. Extraction Methods, Quantitative and Qualitative Phytochemical Screening of Medicinal Plants for Antimicrobial Textiles: A Review. Plants (Basel). 2022 Jul 25;11(15):2011. https://doi.org/10.3390/plants11152011.
41. Pawarti N, Iqbal M, Ramdini DA, Yuliyanda C. The effect of extraction methods on percent yield and phenolic content of plant extracts potentially as antioxidants. Med Prof J Lampung. 2023;13(4):590-593. https://doi.org/10.53089/medula.v13i4.774.
42. Khodayar S, Shushizadeh MR, Tahanpesar E, Makhmalzadeh BS, Sanaeishoar H. Synthesis and Characterization of Novel pH-Responsive Aminated Alginate Derivatives Hydrogels for Tissue Engineering and Drug Delivery. Curr Org Synth. 2023. https://doi.org/10.2174/0115701794210967231016055949.
43. de Oliveira IR, Dos Santos Gonçalves I, Wallace Dos Santos K, Lança MC, Vieira T, Carvalho Silva J, et al. Biocomposite Macrospheres Based on Strontium-Bioactive Glass for Application as Bone Fillers. ACS Mater Au. 2023;3(6):646-658. https://doi.org/10.1021/acsmaterialsau.3c00048.
44. Colin C, Akpo E, Perrin A, Cornu D, Cambedouzou J. Encapsulation in Alginates Hydrogels and Controlled Release: An Overview. Molecules. 2024 May 30;29(11):2515. https://doi.org/10.3390/molecules29112515.
45. Venkatachalam K, Charoenphun N, Nitikornwarakul C, Lekjing S. Effect of Sodium Alginate Concentration on the Physicochemical, Structural, Functional Attributes, and Consumer Acceptability of Gel Beads Encapsulating Tangerine Peel (Citrus reticulata Blanco 'Cho Khun') Extract. Gels. 2025 Oct;11(10):808. https://doi.org/10.3390/gels11100808.
46. Hariyadi DM, Islam N. Current Status of Alginate in Drug Delivery. Adv Pharmacol Pharm Sci. 2020;2020:8886095. https://doi.org/10.1155/2020/8886095.
47. Goh CH, Heng PWS, Chan LW. Alginates as a useful natural polymer for microencapsulation and therapeutic applications. Carbohydr Polym. 2020 Mar 1;231:115682. https://doi.org/10.1016/j.carbpol.2011.11.012
48. Walendziak W, Douglas TEL, Kozlowska J. Design, Optimization, and Characterization of Freeze-Dried Emulsions Based on Sodium Alginate and Whey Protein Isolate Intended for Cosmetic and Dermatological Applications. ACS Omega. 2025;10(23):24932-24949. https://doi.org/10.1021/acsomega.5c02358.
49. Bennacef C, Desobry S, Jasniewski J, Leclerc S, Probst L, Desobry-Banon S. Influence of Alginate Properties and Calcium Chloride Concentration on Alginate Bead Reticulation and Size: A Phenomenological Approach. Polymers (Basel). 2023 Oct 12;15(20):4163. https://doi.org/10.3390/polym15204163.
50. Tomić SL, Babić Radić MM, Vuković JS, Filipović VV, Nikodinovic-Runic J, Vukomanović M. Alginate-Based Hydrogels and Scaffolds for Biomedical Applications. Mar Drugs. 2023 Mar 4;21(3):177. https://doi.org/10.3390/md21030177.
51. Matulyte I, Kasparaviciene G, Bernatoniene J. Development of New Formula Microcapsules from Nutmeg Essential Oil Using Sucrose Esters and Magnesium Aluminometasilicate. Pharmaceutics. 2020 Jul 1;12(7):628. https://doi.org/10.3390/pharmaceutics12070628.
52. Maslii Y, Herbina N, Dene L, Ivanauskas L, Bernatoniene J. Development and Evaluation of Oromucosal Spray Formulation Containing Plant-Derived Compounds for the Treatment of Infectious and Inflammatory Diseases of the Oral Cavity. Polymers (Basel). 2024 Sep 12;16(18):2649. https://doi.org/10.3390/polym16182649.
53. Drapińska P, Skulmowska-Polok K, Chałupka J, Sikora A. Sustained-Release Oral Delivery of NSAIDs and Acetaminophen: Advances and Recent Formulation Strategies-A Systematic Review. Pharmaceutics. 2025 Sep 26;17(10):1264. https://doi.org/10.3390/pharmaceutics17101264

Received: *07-03-2026* - ***Accepted***: *06-05-2026* - ***Published***: *12-05-2026*

54. Biji CA, Balde A, Kim SK, Nazeer RA. Optimization of alginate/carboxymethyl chitosan microbeads for the sustained release of celecoxib and attenuation of intestinal inflammation in vitro. Int J Biol Macromol. 2024 Dec;282(Pt 3):137022. https://doi.org/10.1016/j.ijbiomac.2024.137022.
55. Sıçramaz H, Dönmez AB, Güven B, Ünal D, Aşbay E. Microstructure and Release Behavior of Alginate-Natural Hydrocolloid Composites: A Comparative Study. Polymers (Basel). 2025 Feb 18;17(4):531. **https://doi.org/10.3390/polym17040531**
56. Weng Y, Ranaweera S, Zou D, Cameron AP, Chen X, Song H, et al. Improved enzyme thermal stability, loading and bioavailability using alginate encapsulation. Food Hydrocoll. 2022;137:108385. https://doi.org/10.1016/j.foodhyd.2022.108385.
57. Oyeniyi YJ, Momoh AM. Formulation development of an herbal hand sanitizer containing Moringa olifera silver nanoparticles. Braz J Technol. 2021;4(1):36-49. https://doi.org/10.38152/bjtv4n1-003.
58. Binsuwaidan R, Sultan AA, Negm WA, Attallah NGM, Alqahtani MJ, Hussein IA, Shaldam MA, El-Sherbeni SA, Elekhnawy E. Bilosomes as Nanoplatform for Oral Delivery and Modulated In Vivo Antimicrobial Activity of Lycopene. Pharmaceuticals (Basel). 2022 Aug 24;15(9):1043. https://doi.org/10.3390/ph15091043
59. Korsmeyer RW, Gurny R, Doelker E, Buri P, Peppas NA. Mechanisms of solute release from porous hydrophilic polymers. Int J Pharm. 1983 May;15(1):25-35. https://doi.org/10.1016/0378-5173(83)90064-9
60. Higuchi T. Mechanism of sustained-action medication. Theoretical analysis of the rate of release of solid drugs dispersed in solid matrices. J Pharm Sci. 1963 Dec;52:1145-9. https://doi.org/10.1002/jps.2600521210.
61. Peppas NA. Analysis of Fickian and non-Fickian drug release from polymers. Pharm Acta Helv. 1985;60(4):110-111.
62. Atanu FO, Idih FM, Nwonuma CO, Hetta HF, Alamery S, El-Saber Batiha G. Evaluation of Antimalarial Potential of Extracts from Alstonia boonei and Carica papaya in Plasmodium berghei-Infected Mice. Evid Based Complement Alternat Med. 2021;2021:2599191. https://doi.org/10.1155/2021/2599191.
63. Okpe O, Habila N, Ikwebe J, Upev VA, Okoduwa SI, Isaac OT. Antimalarial Potential of Carica papaya and Vernonia amygdalina in Mice Infected with Plasmodium berghei. J Trop Med. 2016;2016:8738972. https://doi.org/10.1155/2016/8738972.
64. Zeleke G, Kebebe D, Mulisa E, Gashe F. In Vivo Antimalarial Activity of the Solvent Fractions of Fruit Rind and Root of Carica papaya Linn (Caricaceae) against Plasmodium berghei in Mice. J Parasitol Res. 2017;2017:3121050. https://doi.org/10.1155/2017/3121050.
65. Habte G, Tamiru S, Eyasu K. In vivo antimalarial activity of the 80% methanolic crude fruit extract of Lagenaria siceraria (Molina) Standl. against Plasmodium berghei infected mice. Heliyon. 2023 Apr;9(4):e15453. https://doi.org/10.1016/j.heliyon.2023.e15453.
66. Bashir A, Bello MI, Mahmoud SJ, Zailani AH. Antimalarial activity of decoction from Carica papaya, Psidium guajava, and Mangifera indica leaves in mice infected with Plasmodium berghei (NK-65). FUDMA J Sci. 2024;8(3):477-486. https://doi.org/10.33003/fjs-2024-0803-2502.
67. Oraebosi MI, Good GM. Carica papaya augments anti-malarial efficacy of artesunate in Plasmodium berghei parasitized mice. Ann Parasitol. 2021;67(2):295-303. https://doi.org/10.17420/ap6702.342.
68. Indradi RB, Muhaimin M, Barliana MI, Khatib A. Potential Plant-Based New Antiplasmodial Agent Used in Papua Island, Indonesia. Plants (Basel). 2023 Apr 27;12(9):1813. https://doi.org/10.3390/plants12091813.

Received*: 07-03-2026 -* ***Accepted****: 06-05-2026 -* ***Published****: 12-05-2026*